

1 **Airflow reversal and alternating corkscrew vortices in foredune wake zones**
2 **during perpendicular and oblique offshore winds**

3

4 Derek W.T. Jackson¹, Meiring Beyers², Irene Delgado-Fernandez³, Andreas C.W.
5 Baas⁴, Andrew J. Cooper¹, Kevin Lynch⁵

6

7 ¹Centre for Coastal and Marine Research, School of Environmental Science,
8 University of Ulster, Coleraine BT52 1SA, Northern Ireland, United Kingdom

9 ²Klimaat Consulting & Innovation, 49 Winston Crescent, Guelph, ON, Canada N1E

10 2K1

11 ³Natural, Geographical & Applied Sciences, Edge Hill University, St. Helens Road,
12 Ormskirk L39 4QP, England, United Kingdom

13 ⁴Department of Geography, King's College London, Strand, London WC2R 2LS,
14 United Kingdom

15 ⁵Department of Geography, National University of Ireland, Galway, Ireland

16

17 **Abstract**

18 On all sandy coastlines fringed by dunes, understanding localised air flow allows us
19 to examine the potential sand transfer between the beach and dunes by wind-blown
20 (Aeolian) action. Traditional thinking into this phenomenon had previously included
21 only onshore winds as effective drivers of this transfer. Recent research by the
22 authors, however, has shown that offshore air-flow too can contribute significantly,
23 through lee-side back eddies, to the overall windblown sediment budget to coastal
24 dunes. Under rising sea levels and increased erosion scenarios, this is an important
25 process in any post-storm recovery of sandy beaches. Until now though, full

26 visualisation in 3D of this newly recognised mechanism in offshore flows has not
27 been achieved. Here, we show for the first time, this return flow eddy system using
28 3D *computational fluid dynamics* modelling, and reveal the presence of complex
29 corkscrew vortices and other phenomena. The work highlights the importance of
30 relatively small surface undulations in the dune crest which act to induce the spatial
31 patterns of airflow (and transport) found on the adjacent beach.

32

33 **Keywords**

34 Computational fluid dynamics; Aeolian; Foredunes; Transport; Airflow modelling; Lee
35 side eddies

36

37 **1. Introduction**

38 In the calculation of sediment budgets within beach and foredune environments,
39 there is a fundamental requirement to isolate those wind events capable of aeolian
40 sediment transport from the beach (sediment source area) to the adjacent coastal
41 dune field (sink area) (Anthony et al., 2007 and Delgado-Fernandez and Davidson-
42 Arnott, 2011). Until recently, sediment budget calculations (e.g. Fryberger and Dean,
43 1979 and Illenberger and Rust, 1988) often rejected offshore wind as a contributing
44 component. Extensive aeolian dunes on coasts where the dominant wind direction is
45 offshore (leeside coasts) therefore created a research conundrum within traditional
46 thinking in foredune morphodynamics — why should they exist under low forcing
47 conditions? Conventionally, the evolution of these features has been explained away
48 by concluding that regional shifts in wind regime must have occurred (Shennan and
49 Andrews, 2000). It is recognised however, that even though onshore wind directions
50 may in some cases represent the minority of winds at a site; their influence can be

51 significant in providing the bulk of the transport-capable winds feeding local foredune
52 sediment budgets. Offshore winds though can still represent an important
53 supplemental part of the total transport system forming foredunes.

54 Recently, a number of studies on complex interactions between wind and surface
55 topography have provided new insights into important localised steering effects
56 (Lynch et al., 2008, Lynch et al., 2010, Lynch et al., 2013, Delgado-Fernandez et al.,
57 2011, Delgado-Fernandez et al., accepted for publication, Jackson et al.,
58 2011 and Bauer et al., 2012). Research in desert dunes (Frank and Kocurek,
59 1996a, Frank and Kocurek, 1996b and Baddock et al., 2007) and wind tunnels
60 (Walker and Nickling, 2003) indicates that airflow traversing dunes can result in a
61 large range of turbulent processes in their lee-sides, usually in the form of flow
62 separation and re-attachment, deflected flow and reversed eddies, or complex roller
63 vortices or roller helices (Walker and Nickling, 2002). A similar set of flow
64 characteristics can also be applied to coastal foredunes (Bauer et al., 2012). Shear
65 stress within turbulent flows in any of these environments has an inherent
66 heterogeneity which, in turn, can help sustain initiation of sand particles from the
67 surface (Baas and Sherman, 2005). In these conditions, winds that are normally
68 predicted to be sub-threshold in the movement of dry sand may not necessarily halt
69 transport (Wiggs et al., 1996). Examining the intricacies of flow behaviour across
70 such environments therefore is paramount in understanding additional transport
71 potential in sediment budget calculations of beach–dune systems (Jackson et al.,
72 2011).

73 Until recently, field investigations of airflow and sediment transport dynamics during
74 offshore wind conditions, was hampered by shortfalls in technical capabilities of
75 measurement equipment. However, advances in wind modelling and ultrasonic

76 anemometry have resulted in field experiments where landward aeolian sediment
77 transport from local topographic steering of offshore directed airflow has been
78 quantified (Lynch et al., 2008, Lynch et al., 2010 and Lynch et al., 2013). These
79 mechanisms have been shown to play an important role in post-storm recovery of
80 foredunes scarped by wave action, effectively returning displaced sediment back
81 onto the foredune toe and rebuilding the back beach again. Up until these
82 investigations (e.g. Lynch et al., 2008) significant under-estimation of predicted
83 sediment input to the foredune had likely been commonplace. The recent work
84 of Delgado-Fernandez et al. (2011, 2012) also showed that the behaviour of the
85 reversed flow varied according to wind direction and antecedent foredune
86 morphology (Lynch et al., 2010). These observed heterogeneous flow patterns may
87 have further added to the reasons why they were previously discounted (Nordstrom
88 et al., 1996 and Walker et al., 2006).

89 Examining the conditions under which offshore winds play a major role in coastal
90 dune dynamics requires adoption of methodologies that are able to resolve airflow in
91 three dimensions to allow changes in wind direction and terrain morphology to be
92 investigated. Indeed, understanding fluid flow behaviour in the lee of dune
93 morphology per se is essential if we are seeking to unravel dune dynamics in
94 general. This applies to dune movement in a range of environments including
95 subaqueous and desert dunes. Complex flow–surface interactions as well as
96 coherent flow structures from antecedent morphology in these environments
97 ultimately require examination and this must be addressed using a number of
98 methodological approaches.

99 Computational fluid dynamics (CFD) models have been widely used in a number of
100 natural settings using both 2-dimensional (Jackson and Hunt, 1975, Castro,

101 1991, Abe et al., 1993, Byrne and Holdo, 1998, Nicholas, 2001 and Safarzadeh et
102 al., 2009) and more recently in 3-dimensional numerical simulations (Lane et al.,
103 2002, Nguyen and Nestmann, 2004, Inkratas et al., 2009 and Feng and Ning, 2010).
104 3-D modelling approaches can give detailed patterns of flow behaviour over non-
105 uniform topography (Lee et al., 2002, Lun et al., 2003 and Stangroom, 2004) and
106 enable a more detailed examination of complex environments such as natural dune
107 forms and associated air-flow over them. To date, mostly 2-D CFD studies have
108 largely been undertaken. Based on PHOENICSTM 3.5 code and using experimental
109 wind tunnel flow measurements obtained by Walker and Nickling (2003), Parsons et
110 al. (2002) validated a 2-D numerical model. General agreement was found between
111 predicted and modelled results, however, significant disagreement in the lower
112 velocities was found at the lee separation zone. Parsons et al. (2004) simulated 2D
113 wind flow over a single idealised transverse dune of different dimensions to examine
114 dune size and re-attachment points. Recently, Wakes et al. (2010) compared basic
115 2-D numerical simulations alongside cup anemometers data and a wind vane at a
116 coastal dune complex in New Zealand. Jackson et al. (2011) were the first to
117 simulate flow in three dimensions over natural coastal dunes and actually compare
118 model results against 3D anemometer results. Smyth et al. (2012) has also further
119 confirmed the outstanding applicability of using CFD in complex dune blowout
120 environments.

121 Three-dimensional CFD allows a much more comprehensive spatial coverage of the
122 wind field in natural settings than could ever be accomplished using just an
123 instrumented approach. Simulations may be used to examine the role of offshore
124 winds under a large range of conditions. The variable output resolution of the CFD
125 model can also be used to guide where field instruments should be deployed for

126 selective data measurement. To date, computing power has been a limiting factor
127 combined with a lack of cross-disciplinary efforts and the logistical problem of
128 collecting suitable field validation data.

129 This paper presents the results of a 3-D CFD modelling study over complex coastal
130 foredune topography using the OpenFoam software. Previous field data
131 comparisons with steady state Reynolds-averaged Navier–Stokes (RANS) and
132 Large Eddy Simulations (LES) solutions of the model already show excellent
133 agreement (Jackson et al., 2011) and therefore no detailed comparisons will be
134 presented here. The aim of this paper is to highlight for the first time, the three
135 dimensional nature of secondary airflow within this important interface wake zone
136 between the beach and the dune system. The objectives are: 1) to explore possible
137 causes for the spatial variability found during field measurements of foredune wake
138 zones under offshore wind conditions; 2) to isolate the potential effects of terrain
139 form, roughness and wind directional effects; 3) explore the importance of
140 undulations in the foredune crest in dictating the positioning of the detached flow as
141 it rejoins the beach surface again; and 4) compare against field data to help quality
142 check the model results.

143

144 **2. Methods**

145 **2.1. Computational fluid dynamics (CFD) simulations**

146 For the simulations presented here, the open source CFD software OpenFoam®
147 (version 1.7.1) was used. This model makes use of Reynolds-averaged Navier–
148 Stokes (RANS) equations which are time-averaged equations of motion for fluid flow
149 where an instantaneous quantity is decomposed into its time-averaged and
150 fluctuating quantities (Launder and Spalding, 1974). Through using the RANS

151 simulation solver it allowed more simulation tests to be performed quickly. Overall,
152 the simulation of airflow in the study is similar to the modelling approach that yielded
153 favourable comparison to earlier field tests measurements by the authors. More
154 extensive details on the CFD simulation methodology followed can be found
155 in Jackson et al. (2011).

156 **2.2. Re-attachment zone characterisations**

157 To evaluate the spatial extent of the simulated re-attachment zone, the resolved U
158 (horizontal) and W (vertical) velocity components obtained from the CFD field
159 solution were combined in an $\text{atan2}(W/U)$ function to produce the angle between
160 reversed or re-attached horizontal flow in the wake zone and the vertical flow
161 component. This helps with highlighting and visualising the position of the flow re-
162 attachment position behind the foredune. Function values between zero and π
163 indicate re-attached flow, values between $-\pi$ and zero indicate the flow reversal
164 zone and the interface between them (the simulated steady state re-attachment
165 position) identified by function values approaching zero. This method is very well
166 suited to CFD simulated three-dimensional wind flow fields as it can provide a clear
167 three-dimensional spatial visualisation of the foredune flow characteristics not
168 possible with field measurements.

169 **2.3. Surface topography of actual terrain**

170 Using a combination of aerial LiDAR data (spot interval distance of 4 m) and dGPS
171 survey points (spot distance of 1 m across the beach and dune and 0.2 m over the
172 crestral ridge of the foredune) a detailed topographical mesh was created measuring
173 150 m (longshore) \times 250 m (cross-shore) incorporating the main foredune ridge
174 (see Fig. 3). Surveyed points were gridded-up using standard interpolation

175 techniques (kriging) and used as the underlying surface for any wind flow simulations
176 over real terrain.

177

178 **3. Results**

179 **3.1. Artificial dune topography simulations**

180 Prior to performing the simulations for the real terrain where the field wind
181 measurements were conducted, a set of exploratory simulations were carried out for
182 an artificial dune topography, one that mimics the real dune form but where terrain
183 parameters could be altered and tested more readily. The results of these
184 simulations were used to qualitatively isolate the effects of modelled terrain surface
185 roughness; wind direction and dune crest form perturbations. The first simulations
186 were performed to test whether the artificial dune form could qualitatively reproduce
187 a similar spatial extent of the wake zone, as measured and simulated in earlier
188 work. Fig. 1 shows the geometry and results of the first simulation for an offshore
189 wind perpendicular to the dune orientation. Approaching wind flow characteristics
190 included an inlet wind speed of 15 m s^{-1} , surface aerodynamic roughness of 0.01 m
191 and inlet flow profiles and turbulence characteristics as per Richards and Hoxey
192 (1993). The flow reversal zone was visualised with section wind vectors and flow
193 streamlines (shown here) and by plotting the $\text{atan2}(W/U)$ function on an terrain
194 following iso-surface of 1 m above the terrain, as shown in Fig. 1. The flow reversal
195 zone and re-attachment position produced here matched earlier results by Jackson et
196 al. (2011) and Delgado-Fernandez et al. (2011) well. Further tests were conducted to
197 compare results of modelled and explicitly simulated surface roughness effects. This
198 suggested that the modelled surface roughness approach, which uses a typical
199 surface roughness wall function to address the surface shear (Blocken et al., 2007),

200 was adequate, although this was not extensively tested or evaluated here. Lastly, the
201 effects of small intermittent dune crest form perturbations were tested by adding
202 small 0.3 m-high crest extensions on the leeside of the crest. Fig. 2 shows the
203 results of this simulation test which highlights the importance of small terrain effects
204 in producing large (5–10 m) differences in the wake-zone extent. It is important to
205 note that the form and positioning of the crest perturbations were done so that the
206 crest height remained uniform throughout, and that the perturbations are only
207 exposed to the leeside flow and not directly to the approaching and accelerating
208 upstream crest wind flows. As shown in Fig. 2, the intermittent positioning of the
209 leeside crest undulations alters the position of the re-attachment zone significantly.
210 This suggests that crestal surface undulations may be the dominant parameter for
211 the measured wake-zone local spatial variability compared to effects of surface
212 roughness or wind direction

213 **3.2. Airflow simulations over real terrain: perpendicular offshore-directed** 214 **winds**

215 Using detailed terrain data obtained from LiDAR and dGPS surveys, a computational
216 domain was created for the OpenFoam simulations that span the area where field
217 measurements were taken. Fig. 3 shows the Magilligan field test site and resultant
218 terrain and computational domain created for the simulations. Simulations were
219 performed with similar approaching wind flow conditions as for the artificial dune
220 simulations.

221 Magilligan, located in the northern coastline of Northern Ireland, UK was selected
222 because of the numerous studies and datasets accumulated from previous work
223 (e.g. Jackson et al., 2005, Jackson and Cooper, 2010 and Jackson et al., 2011) and
224 not least because of it being located in an exposed windy setting with a predominant

225 offshore wind regime (see insert of Fig. 3). Previous LiDAR and topographical dGPS
226 surveys added to the reasoning for using this site. At Magilligan, the coastline is
227 oriented in a NW–SE axis and runs for approximately 6 km. The beach is up to
228 100 m wide during low tide and has a dissipative, planar topography due to the effect
229 of high energy Atlantic swell waves (Jackson et al., 2005). A microtidal tidal range of
230 approximately 1.6 m operates at the site and beach and foredune sediment is made
231 up of predominantly very well sorted quartz sand with a mean grain diameter of
232 0.17 mm. The foredune ranges in height from 6 to 12 m with dense vegetation
233 dominated by *Ammophila arenaria* of approximately 0.4 m in height. Prevailing winds
234 are from the SW (offshore) and are thought to dominate the aeolian system (Jackson
235 et al., 2011). A section of the beach–dune system was chosen where the foredune
236 crest reaches its highest (10–12 m) and where previous high-frequency wind
237 measurements and CFD modelling have reported airflow separation under offshore
238 winds (Beyers et al., 2010, Delgado-Fernandez et al., 2011 and Jackson et al.,
239 2011).

240 Fig. 4 shows the simulated steady state wind characteristics through a vertical
241 section through the foredune under examination, for a perpendicular offshore-
242 directed wind. The classic wind reversal, re-attachment point and re-attached flow
243 can be observed. When the atan2 function is applied to the simulated 3D flow field,
244 and visualised on a terrain following iso-surface raised 1 m above the terrain surface,
245 the reversed and re-attached flow regimes can be identified, with the re-attachment
246 location the clear boundary between the two.

247 The spatial extent of the reattachment position varies between 35 and 40 m which
248 compares well with the measured re-attachment lengths by Delgado-Fernandez et
249 al. (2011). The extent of the reattachment location varies along the length of the

250 foredune to track the lengthwise dune shape characteristics, and in particular the
251 small variation in height and along wind dune crest positions.

252 When compared to the qualitative simulation of the artificially modified dune crest
253 (Fig. 2) presented earlier, it seems that the flow influences of the small alongshore
254 height variations of the crest matches the flow characteristics of the artificial dune
255 well. Hence, small alongwind variations (~ 0.3 m) of crest position, seems to move
256 the along wind position of the reattachment position by approximately 5 m. This is
257 due to a combination of three-dimensional wind flow effects, and specifically
258 interaction between accelerated flows, delayed crest separation positions and
259 associated leeward reversed flow low pressure areas.

260 Also noteworthy, is that the flow recirculation zone contains at least one classic large
261 flow reversal zone, although the form of the reversal zone is influenced by the
262 presence of the embryo dune shoulder located in the leeward zone.

263 **3.3. Real terrain simulations: oblique offshore-directed winds**

264 Fig. 5 shows a similar steady state simulated wind result for an oblique offshore
265 wind. The wind simulated here approached the foredune at an angle of
266 approximately 45° to the foredune crest orientation. From the sectional views of the
267 flow reversal zone, it can be seen that the reversal zone is now much smaller and
268 mostly isolated within the area between the crest and the leeward dune shoulder.
269 The re-attachment location has also moved closer to the toe of the dune. The
270 oblique flow clearly changes the effective height of the dune and reduces the
271 accelerating effect of the crest separation that reduces the recirculation zone extent.
272 In a few locations along the dune, the reversal zone is only present within the zone
273 between the embryo dune shoulder and the crest, with reattached flow already
274 occurring at the embryo dune toe halfway up the dune slope.

275 Fig. 5 also shows the spatial extent of the flow reversal zones using the atan2
276 method, highlighting the reduction and spatial variation of the separation zone
277 extent. It also shows the reversal zone being isolated to the area between the crest
278 and embryo dune toe. As expected, the flow in the leeward wake is steered to follow
279 the dune crest which results in a corkscrew type vortex that is small in leeward
280 extent from the crest but is stretched downstream along with the steered wind flows.
281 A more complex characteristic of this corkscrew leeward vortex is shown in Fig. 6,
282 identified with streamlines originating windward of the dune crest. The separating
283 flow re-circulates behind the dune and is steered alongshore. Also, as the flow
284 reattaches downstream near the dune toe, the corkscrew vortex re-circulates up and
285 into the embryo dune shoulder/crest recirculation zone. Thus, the upper smaller
286 recirculation zone that is contained in the crest/embryo shoulder zone, receives
287 steered wind flow from the lower dune toe area further upstream. This is different to
288 the more classical flow reversal zone present for perpendicular offshore wind flows,
289 also shown in Fig. 6.

290

291 **4. Discussion**

292 Simulations of surface wind flow over complex foredune topography under offshore–
293 oblique offshore events enables us to unravel the distinctive flow behaviour of the
294 wind according to direction and underlying topographical changes. Simple alterations
295 in the crestal undulations provide a clue to their importance in driving changes in the
296 lateral extent of the re-attachment zone. The positioning of the re-attachment zone
297 itself probably promotes back-beach surface drying through enhanced turbulence
298 and downward flow thereby enhancing the aeolian transport potential of the surface
299 sand, regardless of subsequent events. Through even minor (0.3 m in the vertical)

300 alteration of an artificial 3D foredune crest surface it is clear that this has a significant
301 effect on re-attachment position; significantly shifting the position of this zone. The
302 natural undulations found on a foredune crest therefore give rise to a distinctive
303 heterogeneity in flow re-attachment positioning at the back-beach zone as a result. It
304 might, therefore, be expected that secondary airflow heterogeneity, controlled by
305 small alongshore height variations in crestal topography, would be reflected in
306 sediment transport patterns on the leeside, with the extent of beach where sediment
307 maybe recycled back towards the dune, varying alongshore. Recent results
308 from Lynch et al. (2013) at the site show the distinct variability in transport patterns
309 on the beach during oblique offshore winds and compliment the heterogeneity in air
310 flow found in the modelling in this study. Bauer et al. (2012) also propose a
311 conceptual model for flow–form interaction over large (> 8 m) foredunes under
312 variable wind approach directions. The study of Bauer et al. helps support the
313 modelling results produced here and demonstrates the crucial role played by the
314 crest line in deflecting flow substantially within lee of the foredunes.

315 The results in this study show that incident approach angle of the wind to foredune
316 topography clearly dictates the resulting flow behaviour inside the wake zone of the
317 foredune ridge. With CFD simulations we can observe two distinct flow patterns
318 according to approach (incident) wind angle. First, directly offshore winds have a
319 relatively more ‘simplistic’ behaviour, with a detached flow at the crest and a return
320 eddy in the lee. Flow then reattaches at the reattachment point on the back beach.

321 Secondly, with oblique offshore winds a clear corkscrew vortex is induced in the
322 wake zone, producing complex flow patterns over the surface. At Magilligan the
323 presence of dune vegetation largely restricts the surface sand in its movement,
324 however, further out from the dune toe and still inside the wake zone, the corkscrew

325 is likely to still influence surface sediment mobility. If, for example, the downward
326 twist (or trough) of the corkscrew eddy is coincident with the ground then this will
327 push surface sand landward at this contact point. Back along its length, the 'crest' of
328 the corkscrew vortex will be elevated above the surface at a height that will be less
329 influential in driving sand transport. This will produce onshore and offshore transport
330 patterns on the back beach and foredune zone, enhancing the heterogeneity of the
331 transport surface during oblique offshore wind events. With changes in incident wind
332 direction, the relative position of the corkscrew will probably change alongshore and
333 therefore add to sediment transport heterogeneity, producing fluctuations in transport
334 activity during offshore flow conditions. It is therefore plausible that oblique wind
335 flows, and its resulting cork-screw vortex that alternates into upper and lower
336 recirculation zones, may present an important mechanism in the evolution of
337 foredune form, somewhat different to the effects of classic perpendicular wind flow
338 reversal geomorphic mechanisms.

339 Quantification of transport in the wake zone of foredunes at the beach–dune toe area
340 using standard sand-trapping techniques under the above conditions could prove
341 problematic. Fluctuating flow direction and resultant transport pathways from
342 corkscrew activity will probably lead to under-estimation of actual transport rates
343 occurring. Omni-directional trap design based on Jackson (1996) will help avoid this
344 problem. In other dune types such as desert dunes and where upwind topography is
345 not influencing airflow substantially, we can deduce that transport activity is likely to
346 follow the direction of incident airflow on the stoss face whereas in the wake
347 transport patterns will alternate according to corkscrew and other flow behaviour
348 increasing the complexity in transport patterns as a result.

349

350 **5. Conclusions**

351 The first and rather obvious observation is that small perturbations in the crest
352 position and height can create significant differences in the spatial extent of the
353 leeward recirculation zone attachment position. Within natural foredune ridge
354 topography we generally find a large variability in crest height, undulating according
355 to natural depositional or erosional patterns during its formational history. A second
356 and more interesting observation is that oblique wind flows create more complex
357 three-dimensional corkscrew vortices that are steered alongshore, alternating
358 position between upper crest-to-embryo toe circulation zones and crest-to-lower toe
359 dune positions. These findings have important implications in our attempts at
360 understanding aeolian sediment transport on the back beach and mid-beach zones
361 under variable offshore wind events and highlights the role played by adjacent
362 foredune topography in dictating flow conditions at the back beach. It also
363 emphasises the important role that CFD can play in our understanding of wind flow
364 dynamics over complex geomorphological landforms at a variety of scales, and
365 shows for the first time the presence of corkscrew vortices operating in the wake of
366 foredune morphology. Wake zone airflow (of dunes) is inherently more complex than
367 that of their stoss slopes and the presence of large scale corkscrew vortices will
368 dictate variable aeolian transport conditions in each of these zones as a result. The
369 stoss slope transport will likely follow incident wind direction, whereas wake zone
370 transport will follow complex corkscrew vortex ground contact behaviour and be in
371 tangential directions to stoss transport.

372

373 **Acknowledgements**

374 The authors would like to thank Bernie Bauer and an anonymous reviewer for their
375 constructive comments which helped improve the paper. This work is funded through
376 the UK Natural Environment Research Council grant NE/F019483/1.

377

378 **References**

379

380 Abe, K., Nagano, Y., Kondoh, T., 1993. Numerical simulations of separating and
381 reattaching flows with a modified low-Reynolds-number k - ϵ model. *Journal of*
382 *Wind Engineering and Industrial Aerodynamics*, 46–47 (1993), pp. 85–94

383 Anthony, E.J., Vanhee, S., Ruz, M.-H., 2007. Embryo dune development on a large,
384 actively accreting macrotidal beach: Calais, North Sea coast of France. *Earth*
385 *Surface Processes and Landforms*, 32 (2007), pp. 631–636

386 Baas, A.C.W., Sherman, D.J., 2005. Formation and behavior of Aeolian streamers.
387 *Journal of Geophysical Research — Earth Surface*, 110 (2005)
388 <http://dx.doi.org/10.1029/2004JF000270>

389 Baddock, M.C., Livingstone, I., Wiggs, G.F.S., 2007. The geomorphological
390 significance of airflow patterns in transverse dune interdunes.
391 *Geomorphology*, 87 (2007), pp. 322–336

392 Bauer, B.O., Davidson-Arnott, R.G.D., Walker, I.J., Hesp, P.A., Ollerhead, J., 2012.
393 Wind direction and complex sediment transport response across a beach–
394 dune system. *Earth Surface Processes and Landforms*, 37 (15) (2012), pp.
395 1661–1677

396 Beyers, M., Jackson, D.W.T., Lynch, K., Cooper, J.A.G., Baas, A.C.W., Delgado-
397 Fernandez, I., Pierre-Olivier, D., 2010. Field testing and CFD LES simulation

398 of offshore wind flows over coastal dune terrain in Northern Ireland. The Fifth
399 International Symposium on Computational Wind Engineering (CWE2010),
400 International Association for Wind Engineering, Chapel Hill, North Carolina,
401 USA (2010)

402 Blocken, B., Stathopoulos, T., Carmeliet, J., 2007. CFD simulation of the
403 atmospheric boundary layer: wall function problems. *Atmospheric*
404 *Environment*, 41 (2) (2007), pp. 238–252

405 Byrne, C.E.I., Holdo, A.E., 1998. Effects of increased geometric complexity on the
406 comparison between computational and experimental simulations. *Journal of*
407 *Wind Engineering and Industrial Aerodynamics*, 73 (1998), pp. 159–179

408 Castro, I., 1991. Air flow and sand transport over sand dunes. *Acta Mechanica*
409 *Supplement*, 2 (1991), pp. 1–22

410 Delgado-Fernandez, I., Davidson-Arnott, R.G.D., 2011. The nature of aeolian
411 transport events in coastal areas. *Geomorphology*, 126 (2011), pp. 217–232

412 Delgado-Fernandez, I., Jackson, D.W.T., Cooper, J.A.G., Baas, A.C.W., Lynch, K.
413 Beyers, J.H.M., 2011. Re-attachment zone characterisation under offshore
414 winds blowing over complex foredune topography. *Journal of Coastal*
415 *Research*, SI 64 (1) (2011), pp. 273–277

416 Delgado-Fernandez, I., Jackson, D.W.T., Cooper, J.A.G., Baas, A.C.W., Beyers,
417 J.H.M., Lynch, K., accepted for publication. Field characterization of three-
418 dimensional lee-side airflow patterns under offshore winds at a beach–dune
419 system. *Journal of Geophysical Research — Earth Surface*.

420 Feng, S., Ning, H., 2010. Computational simulations of blown sand fluxes over the
421 surfaces of complex microtopography. *Environmental Modelling and Software*,
422 25 (2010), pp. 362–367

423 Frank, A.,Kocurek, G., 1996a. Toward a model of airflow on the lee side of aeolian
424 dunes. *Sedimentology*, 43 (1996), pp. 451–458

425 Frank, A.,Kocurek, G., 1996b. Airflow up the stoss slope of sand dunes: limitations of
426 current understanding. *Geomorphology*, 17 (1996), pp. 47–54

427 Fryberger, S.G., Dean, D., 1979. Dune forms and wind regime, in: E.D. McKee (Ed.),
428 A Study of Global Sand Seas, U.S. Geological Survey: Professional Paper,
429 1052 (1979), pp. 141–151

430 Illenberger, W.K., Rust, I.C., 1988. A sand budget for the Alexandria coastal
431 dunefield, South Africa. *Sedimentology*, 35 (1988), pp. 513–521

432 Inkratas, C., Gharabaghi, B., Beltaos, S., Krishnappan, B., 2009. 3-D modelling of
433 ice-covered flows in the vicinity of a deep hole in the east channel of the
434 MacKenzie Delta, NWT. *Canadian Journal of Civil Engineering*, 6 (5) (2009),
435 pp. 791–800

436 Jackson, D.W.T., 1996. A new, instantaneous aeolian sand trap design for field use.
437 *Sedimentology*, 43 (5) (1996), pp. 791–796

438 Jackson, D.W.T., Cooper, J.A.G., 2010. Application of the planform equilibrium
439 concept to natural beaches. *Coastal Engineering*, 57 (2010), pp. 112–123

440 Jackson, P.S., Hunt, J.C.R., 1975. Turbulent wind flow over a low hill. *Quarterly*
441 *Journal of the Royal Meteorological Society*, 101 (1975), pp. 929–955

442 Jackson, D.W.T., Cooper, J.A.G., Del Rio, L., 2005. Geological control on beach
443 state. *Marine Geology*, 216 (2005), pp. 297–314

444 Jackson, D.W.T., Beyers, J.H.M., Lynch, K., Cooper, J.A.G., Baas, A.C.W., Delgado-
445 Fernandez, I., 2011. Three-dimensional wind flow behaviour over coastal
446 dune morphology under offshore winds using Computational Fluid Dynamics

447 (CFD) and ultrasonic anemometry. *Earth Surface Processes and Landforms*,
448 36 (8) (2011), pp. 1113–1124

449 Lane, S.N., Hardy, R.J., Elliott, L., Ingham, D.B., 2002. High-resolution numerical
450 modelling of three-dimensional flows over complex river bed topography.
451 *Hydrological Processes*, 16 (2002), pp. 2261–2272

452 Launder, B.E., Spalding, D.B., 1974. The numerical computation of turbulent flows.
453 *Computer Methods in Applied Mechanics and Engineering*, 3 (2) (1974), pp.
454 269–289

455 Lee, S.J., Lim, H.-C., Park, K.-C., 2002. Wind flow over sinusoidal hilly obstacles
456 located in a uniform flow. *Wind and Structures*, 5 (6) (2002), pp. 515–526

457 Lun, Y.F., Mochida, A., Mutakami, S., Yoshino, H., Shirasawa, T., 2003. Numerical
458 simulation of flow over topographic features by revised k–e models. *Journal of*
459 *Wind Engineering and Industrial Aerodynamics*, 91 (2003), pp. 231–245

460 Lynch, K., Jackson, D.W.T., Cooper, J.A.G., 2008. Aeolian fetch distance and
461 secondary airflow effects: the influence of micro-scale variables on meso-
462 scale foredune development. *Earth Surface Processes and Landforms*, 33
463 (2008), pp. 991–1005

464 Lynch, K., Jackson, D.W.T., Cooper, J.A.G., 2010. Coastal foredune topography as
465 a control on secondary airflow regimes under offshore winds. *Earth Surface*
466 *Processes and Landforms*, 35 (3) (2010), pp. 344–353

467 Lynch, K., Delgado-Fernandez, I., Jackson, D.W.T., Cooper, J.A.G., Baas, A.C.W.,
468 Beyers, J.H.M., 2013. Alongshore variation of aeolian sediment transport on a
469 beach under offshore winds. *Aeolian Research*, 8 (2013), pp. 11–18

470 Nguyen, V.T., Nestmann, F., 2004. Applications of CFD in hydraulics and river
471 engineering. *International Journal of Computational Fluid Dynamics*, 18 (2)
472 (2004), pp. 165–174

473 Nicholas, A.P., 2001. Computational fluid dynamics modelling of boundary
474 roughness in gravel-bed rivers: an investigation of the effects of random
475 variability in bed elevation. *Earth Surface Processes and Landforms*, 26
476 (2001), pp. 345–362

477 Nordstrom, K.F., Bauer, B.O., Davidson-Arnott, R.G.D., Gares, P.A., Carter, R.W.G.,
478 Jackson, D.W.T., Sherman, D.K., 1996. Offshore aeolian transport across a
479 beach: Carrick Finn Strand, Ireland. *Journal of Coastal Research*, 12 (3)
480 (1996), pp. 664–672

481 Parsons, D.R., Wiggs, G.F.S., Walker, I.J., Garvey, B.G., Ferguson, R.I., 2002. Time
482 averaged numerical modeling of airflow over an idealized transverse dune.
483 Proceedings of ICAR5/GCTE-SEN Joint Conference, International Center for
484 Arid and Semiarid Lands Studies, Publication 02–2, Texas Tech University,
485 Lubbock, Texas (2002), p. 261

486 Parsons, D.R., Wiggs, G.F.S., Walker, I.J., Ferguson, R.I., Garvey, B.G., 2004.
487 Numerical modeling of airflow over an idealized transverse dune.
488 *Environmental Modelling & Software*, 19 (2004), pp. 153–162

489 Richards, P.J., Hoxey, R.P., 1993. Appropriate boundary conditions for
490 computational wind engineering models using the k–e turbulence model.
491 *Journal of Wind Engineering and Industrial Aerodynamics*, 46–47 (1993), pp.
492 145–153

493 Safarzadeh, A.A., Neyshabouri, S., Dehkordi, A.N., 2009. 2-D numerical simulation
494 of fluvial hydrodynamics and bed morphological changes, in: T.E. Simos, G.

495 Maroulis (Eds.), *Computational Methods in Science and Engineering*,
496 *Advances in Computational Science*, American Institute of Physics
497 *Conference Proceedings*, 1148 (2) (2009), pp. 739–742

498 Shennan, I., Andrews, J., 2000. Holocene land–ocean interaction and environmental
499 change around the North Sea. Geological Society, London, *Special*
500 *Publications*, 166 (2000)

501 Smyth, T.A.G., Jackson, D.W.T., Cooper, J.A.G., 2012. High resolution measured
502 and modelled three-dimensional airflow over a coastal bowl blowout.
503 *Geomorphology*, 177–178 (2012), pp. 62–73

504 Stangroom, P., 2004. CFD modelling of wind flow over terrain. Unpublished PhD
505 thesis, University of Nottingham, UK.

506 Wakes, S.J., Maegli, T., Dickinson, K.J., Hilton, M.J., 2010. Numerical modelling of
507 wind flow over a complex topography. *Environmental Modelling and Software*,
508 25 (2010), pp. 237–247

509 Walker, I.J., Nickling, W.G., 2002. Dynamics of secondary airflow and sediment
510 transport over and in the lee of transverse dunes. *Progress in Physical*
511 *Geography*, 26 (1) (2002), pp. 47–75

512 Walker, I.J., Nickling, W.G., 2003. Simulation and measurement of surface shear
513 stress over isolated and closely spaced transverse dunes in a wind tunnel.
514 *Earth Surface Processes and Landforms*, 28 (2003), pp. 1111–1124

515 Walker, I.J., Hesp, P.A., Davidson-Arnott, R.G.D., Ollerhead, J., 2006. Topographic
516 steering of alongshore airflow over a vegetated foredune: Greenwich Dunes,
517 Prince Edward Island, Canada. *Journal of Coastal Research*, 22 (5) (2006),
518 pp. 1278–1291

519 Wiggs, G.F.S., Livingstone, I., Warren, A., 1996. The role of streamline curvature in
520 sand dune dynamics: evidence from field and wind tunnel measurements.
521 Geomorphology, 17 (1996), pp. 29–46

522

523 **List of figures**

524

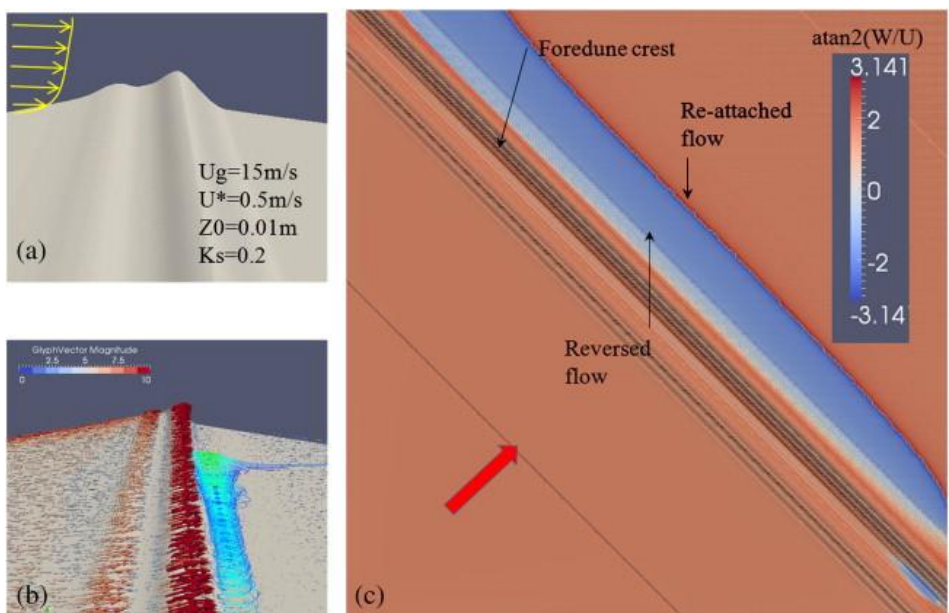


Fig. 1. (a) Artificial dune terrain geometry and approaching flow characteristics to produce a leeward recirculating flow under offshore wind conditions. (b) CFD simulation result of leeward wind flow streamlines and surface velocity vectors 1 m above the terrain. (c) Contour of $\text{atan}2(W/U)$ 1 m above the terrain surface to highlight the extent and boundary between the reversed and re-attached wind flow in foredune wake.

525

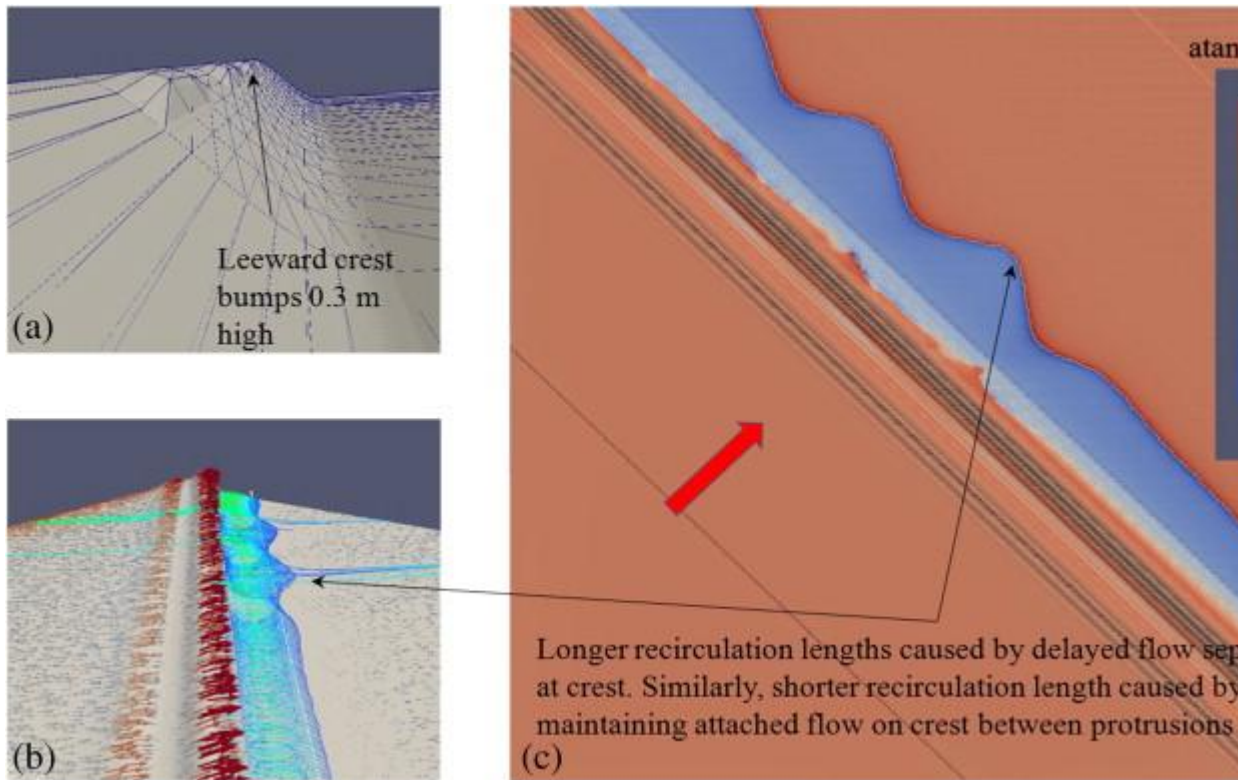


Fig. 2. (a) Close-up of the artificial dune terrain geometry with 0.3 m high leeward dune crest perturbations. (b) CFD simulation result of leeward wind flow streamlines and surface velocity vectors 1 m above the terrain. (c) Contour of $\text{atan2}(W/U)$ 1 m above terrain surface to highlight the extent and boundary between the reversed and re-attached wind flow in foredune wake.

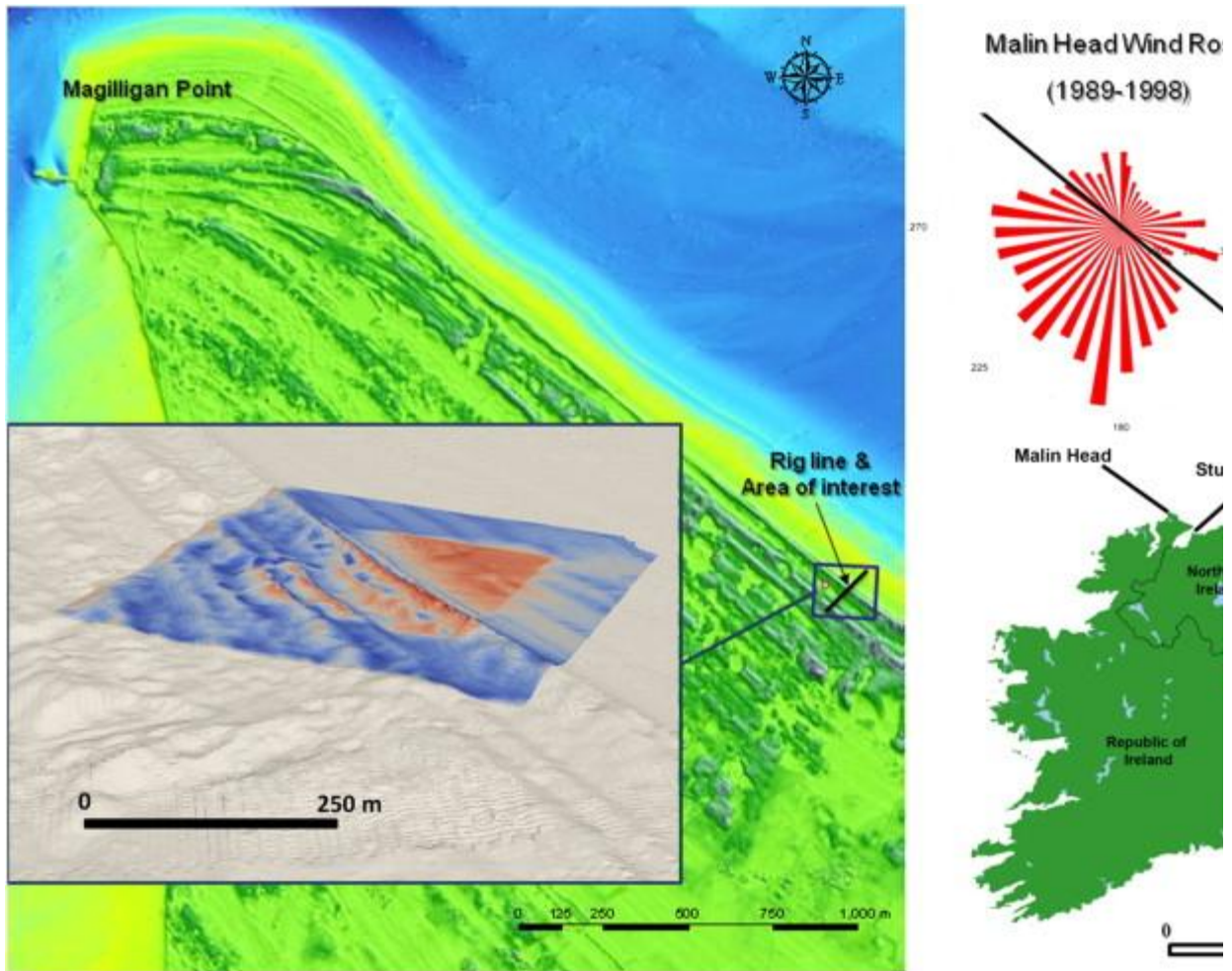
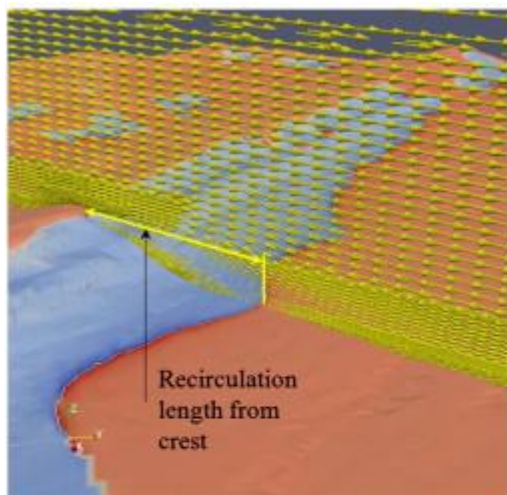


Fig. 3. Location of Magilligan field test site. Insert (left) shows zoomed field test site terrain surface obtained from LiDAR and high resolution dGPS. The colour contour overlay area indicates the horizontal extent of the computational domain created for the CFD simulations. A wind rose for the regional meteorological station at Malin Head is shown (bold black line representing the coastline orientation), demonstrating the dominant offshore winds at Magilligan.



	Field tests	CFD simulation
Recirculation Length	40m - 45m	35m - 40m

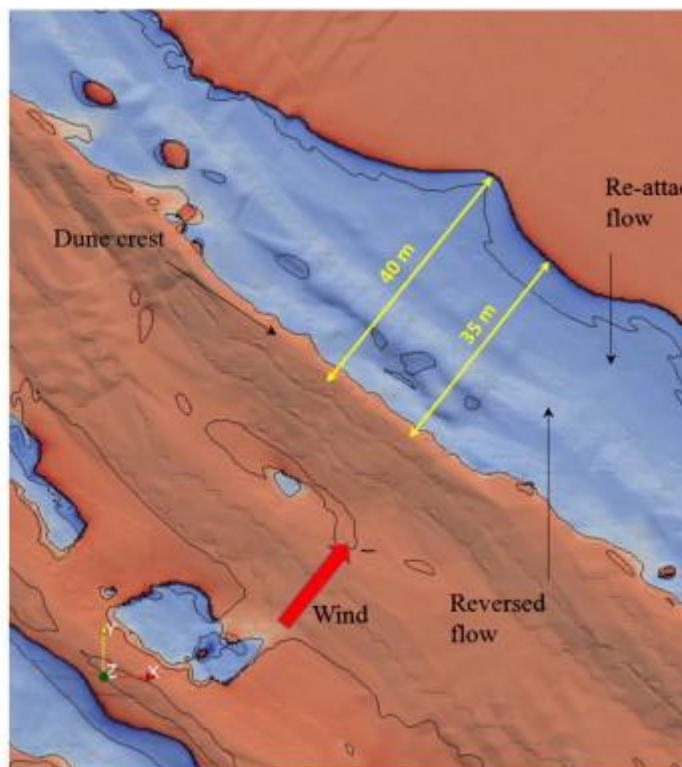
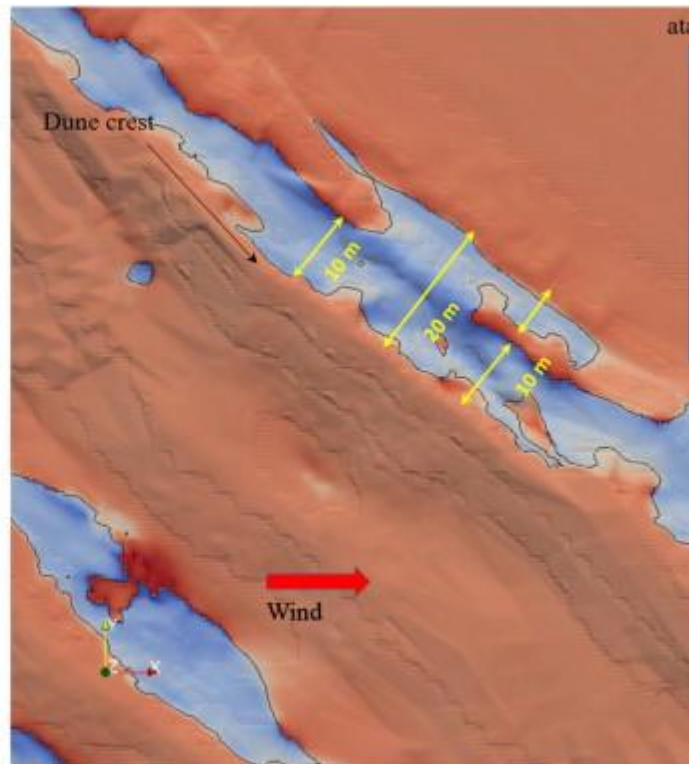
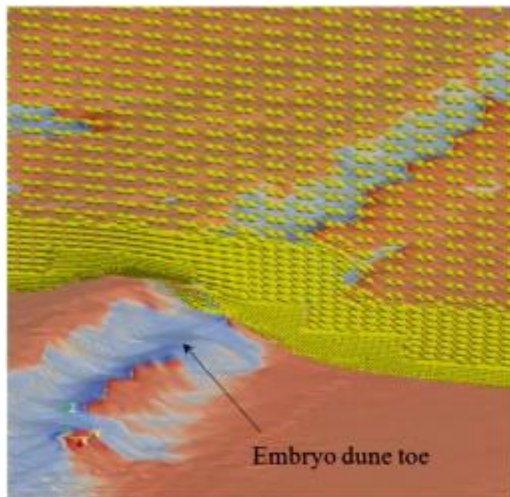


Fig. 4. CFD simulation result for perpendicular offshore wind flow over actual terrain. (Left) Velocity vectors in a vertical plane through the foredune wake zone. (Right) Contours of $\text{atan}2(W/U)$ 1 m above the terrain indicating the extent and separation between the reversed flow and re-attached flow in the dune wake zone.



	Field tests	CFD simulation
Recirculation Length	20m - 25m	10m - 20m

Fig. 5.

CFD simulation result for oblique offshore wind flow over actual terrain. (Left) Velocity vectors in a vertical plane through the foredune wake zone. (Right) Contour of $\text{atan2}(W/U)$ 1 m above the terrain indicating the extent and separation between the reversed flow and re-attached flow in the dune wake zone.

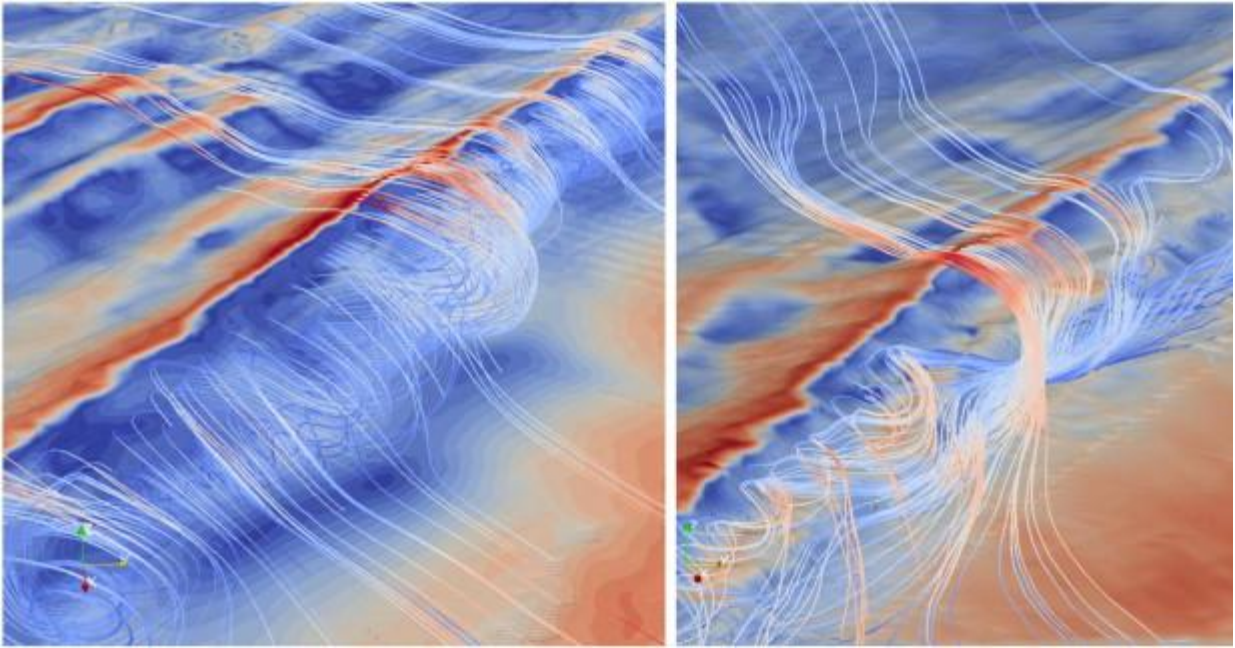


Fig. 6.

Wind flow streamlines in the foredune wake zone under perpendicular offshore winds (left image) and oblique offshore winds (right image) over actual terrain. The wake zone for perpendicular offshore winds shows the classic wake zone characteristics but influenced by the dune crest spatial variations. The oblique offshore wind wake zone shows a corkscrew vortex stretched alongshore by the wind steering. The corkscrew vortex location alternates from the area between the crest to lower dune toe to the area between the crest and embryo dune toe regions.